Prompt J/ψ production in association with a top quark pair at the LHC

Gang Li,[1] Xue-An Pan,[1] Mao Song,[1] and Yu Zhang[2,1,*]

[1]*School of Physics and Materials Science, Anhui University, Hefei 230039, China*

[2]*Institutes of Physical Science and Information Technology, Anhui University, Hefei 230601, China*

(Received 23 May 2019; published 18 October 2019)

In this work, we investigate the prompt J/ψ production in association with a top quark pair to leading order in the nonrelativistic QCD factorization formalism at the LHC with $\sqrt{s} = 13$ TeV. In addition to the contribution from direct J/ψ production, we also include the indirect contribution from the directly produced heavier charmonia χ_{cJ} and ψ'. We present the numerical results for the total and differential cross sections and find that the ${}^3S_1^{(8)}$ states give the dominant contributions. The prompt $t\bar{t}J/\psi$ signatures at the LHC are analyzed in the tetralepton channel $pp \to (t \to W^+(\ell^+\nu)b)(\bar{t} \to W^-(\ell^-\bar{\nu})\bar{b})(J/\psi \to \mu^+\mu^-)$ and trilepton channel $pp \to (t \to W(qq')b)(t \to W(\ell\nu)b)(J/\psi \to \mu^+\mu^-)$, with the J/ψ mesons decaying into a muon pair, and the top quarks decaying leptonically or hadronically. We find that $t\bar{t}J/\psi$ production can be potentially detected at the LHC, whose measurement is useful to test the heavy quarkonium production mechanism.

DOI: 10.1103/PhysRevD.100.074019

I. INTRODUCTION

The nonrelativistic QCD (NRQCD) [1] provides a rigorous theory to study heavy-quarkonium physics, where the production cross section and decay rates can be divided into short-distance and long-distance parts. The short-distance coefficients are process-dependent which can be calculated perturbatively in QCD as expansions in the strong-coupling constant α_s. The long-distance matrix elements (LDMEs) are process-independent and universal which are governed by nonperturbative QCD dynamics and can be extracted from experiments. The relative importance of the LDMEs can be estimated by means of the velocity-scaling rules [2]; i.e., the LDMEs can be classified with a definite power of the relative velocity v of heavy quarks in the bound state within the limit $v \ll 1$. As a result, the theoretical predictions can be expressed as a double series in α_s and v.

The charmonium J/ψ associated-production channels are very important to test the heavy quarkonium physics. At the hadron colliders, such as LHC and Tevatron, there already exist data for $J/\psi + J/\psi$ by LHCb [3,4], D0 [5], CMS [6], and ATLAS [7], $J/\psi + Z$ by ATLAS [8], $J/\psi + W$ by ATLAS [9], J/ψ + charm [10] by LHCb. With the future projected LHC luminosities, more data can be available. On the theoretical side, many efforts have been made for the associated-hadroproduction channels, $J/\psi + J/\psi$ [11–16], $J/\psi + Z$ [17–20], $J/\psi + W$ [17,21,22], $J/\psi + \gamma$ [23–25], J/ψ + charm [26–29], J/ψ + bottom [30,31], where some can be known up to next-to-leading-order (NLO) accuracy for the short-distance coefficient.

Top quark, as the heaviest particle in the standard model (SM), plays an important role in deciphering the fundamental interactions, and its studies are currently driven the LHC experiments. At the LHC, top quarks produced in pairs and associated with bosons through strong interactions have started to be accessible, like for example $t\bar{t}\gamma$ [32–34], $t\bar{t}W/Z$ [35–38], and $t\bar{t}H$ [39,40]. With the running of the LHC, more $t\bar{t}$ associated production channels may can be discovered, such as $t\bar{t}$ production in associated with heavy quarkonium which provides a new channel to understand the heavy quarkonium production mechanism and deepen our understanding of the strong interaction. Our analysis in this paper shows that the Fock state ${}^3S_1^{(8)}$ dominates the production of $t\bar{t}J/\psi$, and contributions from other states are marginal, which implicates that this channel can be used to study the Fock state ${}^3S_1^{(8)}$ of J/ψ with tiny pollution due to other states.

In this paper, we plan to study the prompt $J/\psi + t\bar{t}$ production at the LHC in the NRQCD factorization formalism to leading-order (LO). Prompt J/ψ candidates that can also be produced indirectly via radiative or hadronic decays of heavier charmonium states, such as $\chi_{cJ} \to J/\psi + \gamma$ and $\psi' \to J/\psi + X$, are not distinguished from directly produced J/ψ. The respective decay branching ratios are [41] $\mathrm{Br}(\chi_{c0} \to J/\psi + \gamma) = (1.40 \pm 0.05)\%$,

*dayu@nju.edu.cn;dayu@ahu.edu.cn

$\mathrm{Br}(\chi_{c1}\to J/\psi+\gamma)=(34.3\pm1.0)\%$, $\mathrm{Br}(\chi_{c2}\to J/\psi+\gamma)=(19.0\pm0.5)\%$, and $\mathrm{Br}(\psi'\to J/\psi+X)=(61.4\pm0.6)\%$. Contributions to the total $t\bar{t}J/\psi$ production rate can also come from the process of $t\bar{t}+b$-hadrons with weak decays of $b\to J/\psi+X$, which can be separated easily in the detectors. Therefore, we do not consider the J/ψ production through b-hadron decay here.

This paper is organized as follows. In Sec. II, we describe the details of the calculation strategies. In Sec. III, we present the numerical results of the total and differential cross sections for $t\bar{t}J/\psi$ at the production level. In Sec. IV, we analyze $t\bar{t}J/\psi$ signatures at the LHC with the decay of the top quarks and J/ψ. Discussion and summary are given in Sec. V.

II. THE DETAILS OF THE CALCULATION

In this section, we present the details of the calculation for the process $pp\to t\bar{t}+J/\psi$ of prompt J/ψ production associated with top pair at the LHC in the NRQCD factorization formalism to LO. The cross section for the direct production of charmonium state $\mathcal{Q}$ associated with top quark pair $pp\to t\bar{t}+\mathcal{Q}$ can be expressed as

$$\sigma(pp\to t\bar{t}+\mathcal{Q})=\int dx_1dx_2\sum_n\langle\mathcal{O}^{\mathcal{Q}}[n]\rangle\hat{\sigma}(gg\to t\bar{t}+c\bar{c}[n])\times[G_{g/A}(x_1,\mu_f)G_{g/B}(x_2,\mu_f)]. \quad (1)$$

Here $\langle\mathcal{O}^{\mathcal{Q}}[n]\rangle$ is the LDME describing the hadronization of the $c\bar{c}[n]$ pair into the observable quarkonium state $\mathcal{Q}$, n denotes the $c\bar{c}$ Fock states contributing at LO in v, which is specified for $\mathcal{Q}=J/\psi,\psi',\chi_{cJ}$ in Table I, with $J=0,1,2$. From spin symmetry of the heavy quark, the LDMEs at LO in v have the multiplicity relations

$$\begin{aligned}\langle\mathcal{O}^{J/\psi,\psi'}[^3P_J^{(8)}]\rangle&=(2J+1)\langle\mathcal{O}^{J/\psi,\psi'}[^3P_0^{(8)}]\rangle,\\ \langle\mathcal{O}^{\chi_{cJ}}[^3S_1^{(8)}]\rangle&=(2J+1)\langle\mathcal{O}^{\chi_{c0}}[^3S_1^{(8)}]\rangle,\\ \langle\mathcal{O}^{\chi_{cJ}}[^3P_J^{(1)}]\rangle&=(2J+1)\langle\mathcal{O}^{\chi_{c0}}[^3P_0^{(1)}]\rangle.\end{aligned} \quad (2)$$

$G_{g/A,B}(x,\mu_f)$ represent the distribution function at the scale μ_f of gluon which carries the momentum fraction x of the proton A or B.

TABLE I. Values of k in the velocity-scaling rule $\langle\mathcal{O}^{\mathcal{Q}}[n]\rangle\propto v^k$ for the leading $c\bar{c}$ Fock states n pertinent to $\mathcal{Q}$.

k	J/ψ, ψ'	$\chi_{c,J}$
3	$^3S_1^{(1)}$	...
5	...	$^3P_J^{(1)}$, $^3S_1^{(8)}$
7	$^1S_0^{(8)}$, $^3S_1^{(8)}$, $^3P_J^{(8)}$	...

The $\hat{\sigma}(gg\to t\bar{t}+c\bar{c}[n])$ describes the short-distance cross section for the partonic process $g(p_1)+g(p_2)\to t(p_3)+\bar{t}(p_4)+c\bar{c}[n](p_5)$ of a $c\bar{c}$ pair in a Fock state n, and is calculated from the amplitudes using certain projectors onto the usual QCD amplitudes for open $c\bar{c}$ production. The amplitude for $gg\to t\bar{t}+c\bar{c}[n]$ involves 36 Feynman diagrams, which are drawn in Fig. 1 representatively.

The LO short-distance cross section can be obtained by performing the integration over the phase space expressed as below,

$$\hat{\sigma}(gg\to t\bar{t}+c\bar{c}[n])=\frac{(2\pi)^4}{2\hat{s}N_{\mathrm{col}}N_{\mathrm{pol}}}\int\overline{\sum}|\mathcal{A}_{Q\bar{Q}[n]}|^2d\Omega_3. \quad (3)$$

The summation is taken over the spins and colors of initial and final states, and the bar over the summation denotes averaging over the spins and colors of initial partons. The Mandelstam variable $\hat{s}=(p_1+p_2)^2$, is the partonic center-of-mass system energy. N_{col} and N_{pol} refer to the numbers of color and polarization state of $c\bar{c}[n]$. The three-body phase space element can be defined as

$$d\Omega_3=\delta^{(4)}\left(p_1+p_2-\sum_{i=3}^{5}p_i\right)\prod_{j=3}^{5}\frac{d^3\vec{p}_j}{(2\pi)^32E_j}. \quad (4)$$

$\mathcal{A}$ refers to the QCD amplitude with amputated heavy-quark spinors. In the notations of Ref. [42]:

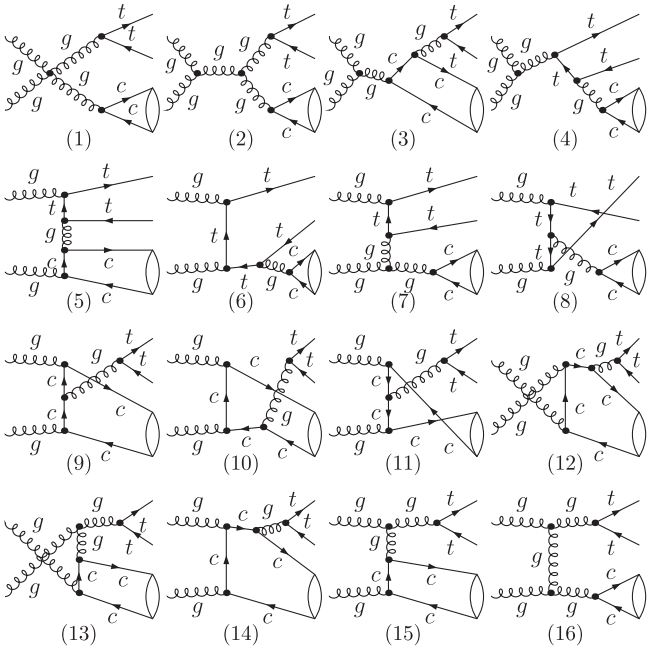

FIG. 1. Representative diagrams at LO for the partonic process $gg\to t\bar{t}+c\bar{c}[n]$.

TABLE II. Total cross section (in unit of fb) of the direct charmonium production process $pp \to t\bar{t} + \mathcal{Q}$ at the 13 TeV LHC with basic cut.

Fock state	$^3S_1^{(1)}$	$^1S_0^{(8)}$	$^3S_1^{(8)}$	$^3P_J^{(8)}$	$^3P_J^{(1)}$	Total
$\sigma(pp \to t\bar{t} + J/\psi)$	0.125	9.57	714.08	17.25	⋯	741.03
$\sigma(pp \to t\bar{t} + \psi')$	0.077	4.79	127.51	4.93	⋯	137.31
$\sigma(pp \to t\bar{t} + \chi_{c2})$	⋯	⋯	701.33	⋯	27.67	729.00
$\sigma(pp \to t\bar{t} + \chi_{c1})$	⋯	⋯	420.80	⋯	43.95	464.75
$\sigma(pp \to t\bar{t} + \chi_{c0})$	⋯	⋯	140.27	⋯	16.23	156.50

$$\begin{aligned}
\mathcal{A}_{Q\bar{Q}[^1S_0^{(1/8)}]} &= \mathrm{Tr}[\mathcal{C}_{1/8}\Pi_0\mathcal{A}]_{q=0},\\
\mathcal{A}_{Q\bar{Q}[^3S_1^{(1/8)}]} &= \varepsilon_\alpha \mathrm{Tr}[\mathcal{C}_{1/8}\Pi_1^\alpha\mathcal{A}]_{q=0},\\
\mathcal{A}_{Q\bar{Q}[^1P_1^{(1/8)}]} &= \varepsilon_\alpha \frac{d}{dq_\alpha}\mathrm{Tr}[\mathcal{C}_{1/8}\Pi_0\mathcal{A}]_{q=0},\\
\mathcal{A}_{Q\bar{Q}[^3P_J^{(1/8)}]} &= \varepsilon_{\alpha\beta}^{(J)} \frac{d}{dq_\beta}\mathrm{Tr}[\mathcal{C}_{(1/8)}\Pi_1^\alpha\mathcal{A}]_{q=0},
\end{aligned} \tag{5}$$

where the lower index q denotes the momentum of the charm-quark in the $c\bar{c}$ rest frame. $\Pi_{0/1}$ are spin projectors onto the spin singlet and spin triplet states. $\mathcal{C}_{1/8}$ are color projectors onto the color-singlet and color-octet states. ε_α and $\varepsilon_{\alpha\beta}$ represent the polarization vector and tensor of the $c\bar{c}$ states, respectively.

III. THE RESULTS AT THE PRODUCTION LEVEL

In this section, we present the numerical results for the production of prompt J/ψ mesons in association with the top pair at the LHC with $\sqrt{s} = 13$ TeV. The masses of the charm quark and top quark are taken as $m_c = 1.5$ GeV and $m_t = 172$ GeV. We use the CTEQ6L1 parton distribution functions [43] with a one-loop running α_s in the LO calculations. Our default choice of factorization scale is $\mu_f = m_T^{\mathcal{Q}}$, where $m_T^{\mathcal{Q}} = \sqrt{(p_T^{\mathcal{Q}})^2 + 4m_c^2}$ is the charmonia $\mathcal{Q}$ transverse mass, and $p_T^{\mathcal{Q}}$ is the charmonia $\mathcal{Q}$ transverse momentum. We apply the cut

$$p_T^{\mathcal{Q}} > 3 \text{ GeV} \tag{6}$$

to the final charmonia, which is defined as the "basic cut" hereafter. We use FeynArts [44] to generate Feynman diagrams and amplitudes for the partonic process $gg \to t\bar{t} + c\bar{c}[n]$. Then the corresponding amplitudes are reduced with FeynCalc [45] and FeynCalcFormLink [46]. At last the numerical calculations are obtained with FormCalc [47].

We adopt the LDMEs for direct J/ψ production from [48,49] as

$$\begin{aligned}
\langle \mathcal{O}^{J/\psi}[^3S_1^{(1)}]\rangle &= 1.1 \text{ GeV}^3,\\
\langle \mathcal{O}^{J/\psi}[^1S_0^{(8)}]\rangle &= 1 \times 10^{-2} \text{ GeV}^3,\\
\langle \mathcal{O}^{J/\psi}[^3S_1^{(8)}]\rangle &= 1.12 \times 10^{-2} \text{ GeV}^3,\\
\langle \mathcal{O}^{J/\psi}[^3P_0^{(8)}]\rangle &= 11.25 \times 10^{-3} \text{ GeV}^5.
\end{aligned} \tag{7}$$

The LDMEs for direct ψ' and χ_{cJ} production and are chosen from [50] and [51,52] as

$$\begin{aligned}
\langle \mathcal{O}^{\psi'}[^3S_1^{(1)}]\rangle &= 0.67 \text{ GeV}^3,\\
\langle \mathcal{O}^{\psi'}[^1S_0^{(8)}]\rangle &= 5 \times 10^{-3} \text{ GeV}^3,\\
\langle \mathcal{O}^{\psi'}[^3S_1^{(8)}]\rangle &= 2 \times 10^{-3} \text{ GeV}^3,\\
\langle \mathcal{O}^{\psi'}[^3P_0^{(8)}]\rangle &= 3.214 \times 10^{-3} \text{ GeV}^5,
\end{aligned} \tag{8}$$

and

$$\begin{aligned}
\langle \mathcal{O}^{\chi_{c0}}[^3S_1^{(8)}]\rangle &= 2.2 \times 10^{-3} \text{ GeV}^3,\\
\langle \mathcal{O}^{\chi_{c0}}[^3P_0^{(1)}]\rangle &= \frac{3N_c}{2\pi} \times 0.075 \text{ GeV}^5,
\end{aligned} \tag{9}$$

with $N_c = 3$. In our calculations, the relations of LDMEs with conventions of Bodwin-Braaten-Lepage have been considered [42].

In Table II, we present the cross section of the direct production of the charmonia $J/\psi, \psi', \chi_{cJ}$ associated with top quark pair at the 13 TeV LHC. We list the contribution from each $c\bar{c}$ Fock state, respectively. It can be seen that the contribution from the Fock state $^3S_1^{(8)}$ is dominant for all the direct production of charmonia J/ψ, ψ', χ_{cJ} in associated with $t\bar{t}$ at the 13 TeV LHC, since it mostly comes from the process of gluon transition. Especially for J/ψ (χ_{c2}), $^3S_1^{(8)}$ state can contribute about 714 (701) fb which is nearly 96.3% (96.2%) of the corresponding total cross section. The summation of cross section for the processes $pp \to t\bar{t}\chi_{cJ}$ with $J = 0$, 1, 2, can reach 1350 fb, which will provide abundant and fascinating studies of phenomenology at the LHC [53].

We summarize the direct and indirect contributions from the radiative or hadronic decays of heavier charmonium states for the prompt J/ψ production in Table III. The cross sections of the four residual indirect production channels can be obtained approximately by multiplying the cross sections of the respective intermediate directly produced charmonium states with their decay branching ratios to J/ψ mesons:

$$\sigma^{\text{indirect}}(\text{From } \psi') = \sigma(pp \to t\bar{t} + \psi') \times \mathrm{Br}(\psi' \to J/\psi + X) \tag{10}$$

TABLE III. Total cross section for J/ψ production from direct and indirect contributions at 13 TeV LHC with basic cut.

Source	From ψ'	From χ_{c2}	From χ_{c1}	From χ_{c0}	Indirect	Direct	Prompt
σ (fb)	84.31	138.51	159.41	2.19	384.42	741.03	1125.45

$$\sigma^{\text{indirect}}(\text{From}\,\chi_{cJ}) = \sigma(pp \to t\bar{t} + \chi_{cJ}) \times \text{Br}(\chi_{cJ} \to J/\psi + \gamma) \tag{11}$$

We can see that the total prompt $t\bar{t}J/\psi$ production rates at the 13 TeV LHC can reach more than 1100 fb, of which the indirect contribution accounts for about 34%. The indirect contribution mainly comes from the $pp \to t\bar{t}\chi_{c2}$ and $pp \to t\bar{t}\chi_{c1}$ channels which can account for nearly 77% of the total indirect contribution. The indirect contribution from χ_{c0} is less than 1%, which can be neglected.

In Fig. 2, we present the distributions of the final J/ψ transverse momentum $p_T^{J/\psi}$ and the rapidity $y_{J/\psi}$ for the direct production process $pp \to t\bar{t} + J/\psi$ at the 13 TeV LHC. For comparison, we also show the Fock states ${}^3S_1^{(1)}$, ${}^1S_0^{(8)}$, ${}^3S_1^{(8)}$, and ${}^3P_J^{(8)}$ there. We can see that the J/ψ spectrum of all the Fock states steadily decrease with the increment of $p_T^{J/\psi}$. In the range of 3 GeV $\leq p_T^{J/\psi} \leq$ 40 GeV, the $d\sigma/dp_T^{J/\psi}$ is in the range of $[0.91, 154.18]$ fb/GeV. We can see that the ${}^3S_1^{(8)}$ state gives the dominant contribution in the whole plotted region, and the curves of total and ${}^3S_1^{(8)}$ state contribution

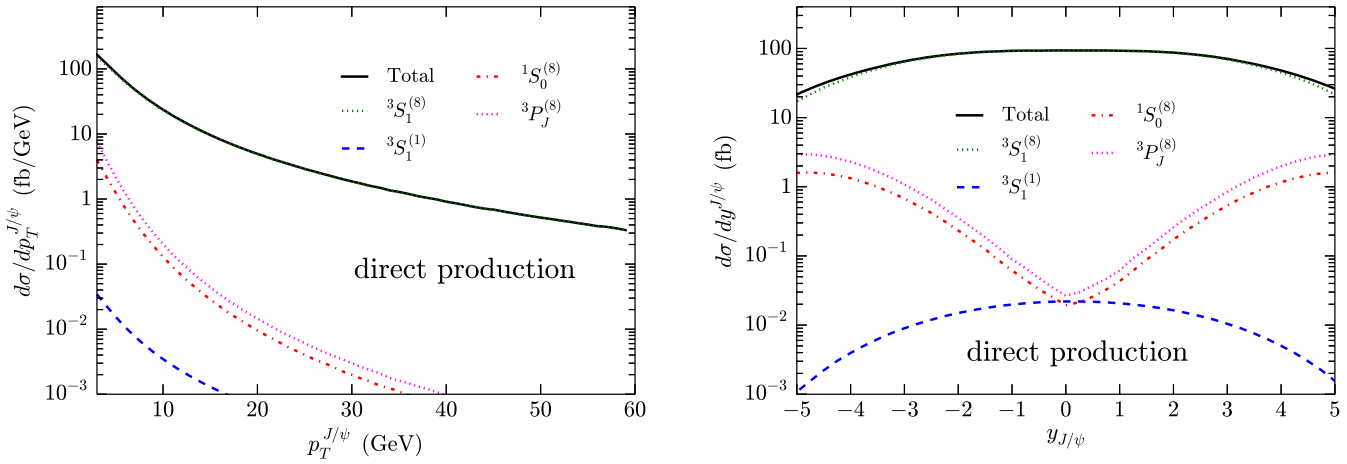

FIG. 2. The LO distributions of $p_T^{J/\psi}$ and $y_{J/\psi}$ for the direct J/ψ production process $pp \to t\bar{t} + J/\psi$ at the 13 TeV LHC. The contributions from Fock states ${}^3S_1^{(1)}$, ${}^1S_0^{(8)}$, ${}^3S_1^{(8)}$, and ${}^3P_J^{(8)}$ are listed, respectively.

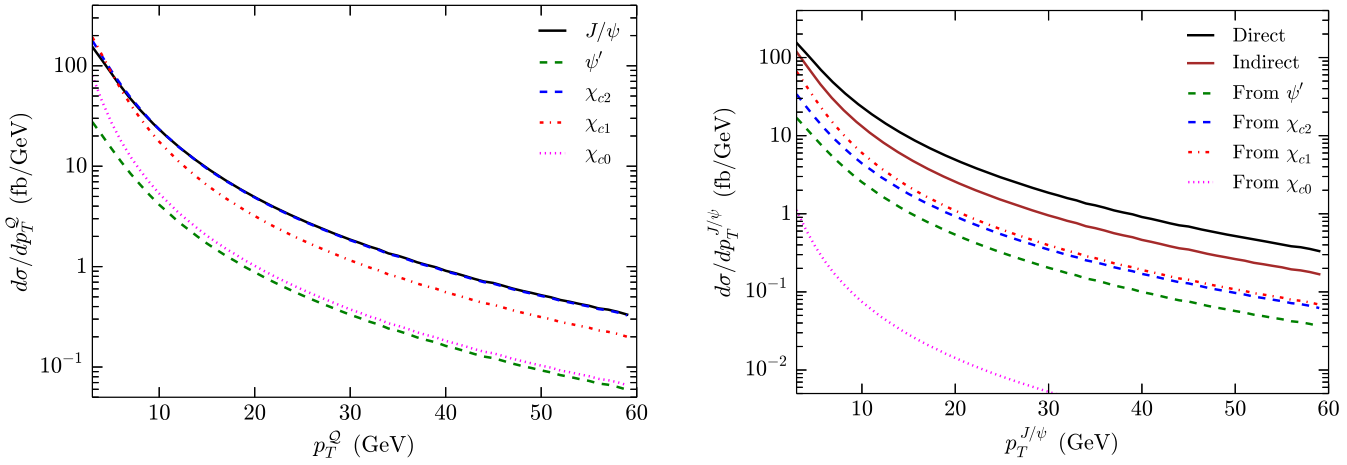

FIG. 3. Left: The LO p_T distributions for the direct charmonia $\mathcal{Q}$ production process $pp \to t\bar{t} + \mathcal{Q}$ at the 13 TeV LHC. Right: The contribution from the direct and indirect J/ψ production for LO $p_T^{J/\psi}$ distributions.

TABLE IV. Total cross sections of the direct J/ψ production process $pp \to t\bar{t} + J/\psi$ at 13 TeV LHC with four different sets of LDMEs, in which Set 1, 2 and 3 are extracted from the polarization of prompt J/ψ at the Fermilab Tevatron [57], hadroproduction of η_c at the LHC [58] and hadroproduction process at the Tevatron [59], respectively. The last column lists the default J/ψ LDMEs [48,49] used in this paper.

	Set 1	Set 2	Set 3	Default set
$\langle \mathcal{O}^{J/\psi}[^3S_1^{(1)}] \rangle$ (GeV^3)	1.4	0.645	0.73	1.1
$\langle \mathcal{O}^{J/\psi}[^1S_0^{(8)}] \rangle$ (GeV^3)	3.3×10^{-2}	0.78×10^{-2}	1×10^{-2}	1×10^{-2}
$\langle \mathcal{O}^{J/\psi}[^3S_1^{(8)}] \rangle$ (GeV^3)	3.9×10^{-3}	1.057×10^{-2}	1.5×10^{-2}	1.12×10^{-2}
$\langle \mathcal{O}^{J/\psi}[^3P_0^{(8)}] \rangle$ (GeV^5)	2.18×10^{-2}	4.3515×10^{-2}	2.25×10^{-2}	11.25×10^{-3}
$\sigma(pp \to t\bar{t} + J/\psi)$ (fb)	331.82	748.16	1000.51	741.03

for the distribution are almost overlapping. For the $y_{J/\psi}$ distributions, at the center region $y_{J/\psi} = 0$, the contributions from $^3S_1^{(1)}$ and $^3S_1^{(8)}$ states reach their maximum, while the contributions from $^1S_0^{(8)}$ and $^3P_J^{(8)}$ states reach their minimum.

The transverse momentum distributions for the direct production charmonia $\mathcal{Q}$ in the channels $pp \to t\bar{t} + \mathcal{Q}$ are shown in the Fig. 3 on the left. We also plot the $p_T^{J/\psi}$ spectra from the indirect contributions in the Fig. 3 on the right. We can find that, at 13 TeV LHC, the p_T distribution for the direct production χ_{c2} and χ_{c1} are larger in the lower p_T region than J/ψ. Besides the Fock state $^3S_1^{(8)}$, which almost contribute all to direct J/ψ production, there are additional contributions from the Fock state $^3P_J^{(1)}$ in χ_{c2} and χ_{c1} direct production. Since the amplitude from the Fock state $^3P_J^{(1)}$ is more orders in terms of $(p_T)^{-2}$ than Fock state $^3S_1^{(8)}$, the steeper distributions of p_T for χ_{c2} and χ_{c1} than J/ψ will be seen. In additional, one can also see that the p_T distribution for χ_{c1} is steeper than χ_{c2}, just because more contributions from the Fock state $^3P_J^{(1)}$. The two curves of p_T distribution for χ_{c2} and J/ψ almost coincide, since their LDMEs of Fock state $^3S_1^{(8)}$, which dominate the contributions, are about the same size. The behavior of the spectra for the direct and indirect contributions are similar; and the indirect contribution from χ_{c0} is much less than other channels in the whole plotted $p_T^{J/\psi}$ region.

As we know, the LDMEs can be extracted from experiments. So far, several sets LDMEs [54–56] of the J/ψ at the NLO based on different experimental processes have been matched by some collaborations. Since only LO NRQCD contributions are considered in this paper, we choose the LDMEs of heavy quarkonium at LO. In order to discuss the uncertainty due to the LDMEs, in Table IV, we show the total cross sections of the direct J/ψ production process $pp \to t\bar{t} + J/\psi$ at 13 TeV LHC with other three different sets of LDMEs, which are extracted from the polarization of prompt J/ψ at the Fermilab Tevatron [57], hadroproduction of η_c at the LHC [58] and hadroproduction process at the Tevatron [59], respectively. We can see that direct J/ψ production cross section varies between 45%–135% compared with the result with default set of LDMEs.

IV. ANALYSES OF $t\bar{t}J/\psi$ SIGNATURES AT THE LHC

In this section, we analyze the prompt J/ψ production associated with top quark pair signatures at the LHC. We focus on the J/ψ decaying into a pair of opposite-sign (OS) muons in $t\bar{t}J/\psi$ production,[1] which presents as irreducible background the $t\bar{t}\mu^+\mu^-$ production. The events for the background $pp \to t\bar{t}\mu^+\mu^-$ are simulated with MADGRAPH [61]. The $J/\psi \to \mu^+\mu^-$ decay is implemented with the narrow width approximation (NWA) method, and event weights are rescaled by the branching ratio $\mathrm{BR}(J/\psi \to \mu^+\mu^-) = 5.961\%$, which is taken from [41].

A. Stable top quarks

We begin our discussion without including top quark decays. For the final muons of the signal and background processes, the following cuts are applied:

$$p_T^{\mu^\pm} > 2.5 \text{ GeV}, |\eta_{\mu^\pm}| < 2.3,$$
$$|m(\mu^+\mu^-) - m_{J/\psi}| < 0.5 \text{ GeV}, \quad (12)$$

where $p_T^{\mu^\pm}$ and $\eta_{\mu^\pm}$ are the transverse momentum and pseudorapidity of the final muon and $m(\mu^+\mu^-)$ denotes the invariant mass of the final muon pair. Using the cuts for J/ψ probed in the ATLAS experiment, additional cuts are also applied to the final reconstructed J/ψ mesons [8,9]:

$$p_T^{J/\psi} > 8.5 \text{ GeV}, \qquad |y_{J/\psi}| < 2.1, \quad (13)$$

where $p_T^{J/\psi}$ and $y_{J/\psi}$ are the transverse momentum rapidity of the J/ψ mesons reconstructed from the muon pair.

[1]The $J/\psi \to e^+e^-$ channel is not used because the ATLAS detector has poor signal efficiency for the J/ψ relevant momentum range [60].

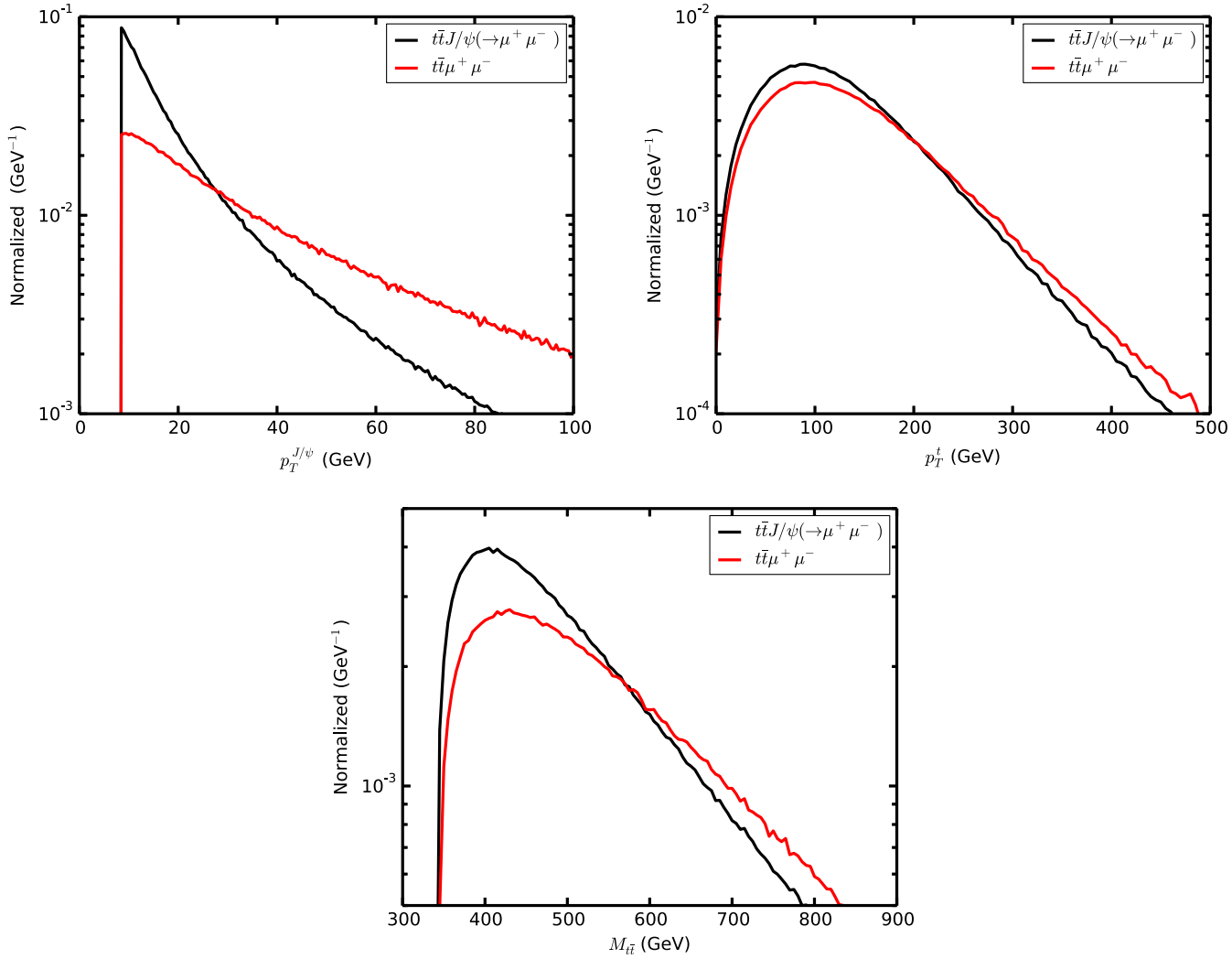

FIG. 4. The normalized distributions of p_T^t and $p_T^{J/\psi}$ and the top quark pair invariant masses $M_{t\bar{t}}$ for the prompt $t\bar{t}J/\psi(\to\mu^+\mu^-)$ and the background $t\bar{t}\mu^+\mu^-$ at the 13 TeV LHC.

In Fig. 4, we display the normalized distributions of the transverse momentum of the final top (p_T^t) and the final reconstructed J/ψ ($p_T^{J/\psi}$) and the top quark pair invariant masses $M_{t\bar{t}}$ for the prompt $t\bar{t}J/\psi(\to\mu^+\mu^-)$ and the background $t\bar{t}\mu^+\mu^-$. We can see that the signal decrease faster than the background with increasing $p_T^{J/\psi}$, $M_{t\bar{t}}$ and p_T^t. In order to increase the significance $\mathcal{S}=S/\sqrt{B}$, where S (B) is the number of signal (background) events, we investigate the $p_T^{J/\psi}$, $M_{t\bar{t}}$, and p_T^t cuts effects, and find that when

$$p_T^{J/\psi} < 30 \text{ GeV}, \tag{14}$$

the significance can be maximized based on the cuts (12) and (13).

In Table V, we present the total cross sections for $t\bar{t}$ associated with the direct and indirect production J/ψ mesons including J/ψ mesons decay to muon pair, and the SM background $pp\to t\bar{t}\mu^+\mu^-$, after each cut above at 13 TeV LHC. In the last column, the corresponding prompt

TABLE V. The cross sections (in unit of fb) for the signal from the direct and prompt J/ψ and background after each cut at the 13 TeV LHC. The significance is given with L = 100 fb^{-1}.

		Indirect						
Cut\Contribution	Direct	From $\psi(2S)$	From χ_{c2}	From χ_{c1}	From χ_{c0}	Total indirect	Background	$\mathcal{S}$
Cut (12)	12.56	1.38	2.37	2.65	0.036	6.44	0.82	209.8
Cut (13)	5.62	0.62	1.05	1.145	0.015	2.83	0.74	98.2
Cut (14)	4.25	0.47	0.79	0.86	0.01	2.13	0.34	109.4

TABLE VI. List of the tetralepton channels for $t\bar{t}J/\psi$ production. The symbols b and ν denote a b-quark or antiquark and neutrino or antineutrino, respectively, with charge conjugation implied.

$t\bar{t}$ decay	J/ψ decay	Channel
$(e^+\nu b)(e^-\bar{\nu}\,\bar{b})$	$\mu^+\mu^-$	$2\mu 2e 2b + \not{E}_T$
$(e^+\nu b)(\mu^-\bar{\nu}\,\bar{b})$	$\mu^+\mu^-$	$3\mu 1e 2b + \not{E}_T$
$(\mu^+\nu b)(e^-\bar{\nu}\,\bar{b})$	$\mu^+\mu^-$	$3\mu 1e 2b + \not{E}_T$
$(\mu^+\nu b)(\mu^-\bar{\nu}\,\bar{b})$	$\mu^+\mu^-$	$4\mu 2b + \not{E}_T$

significance $\mathcal{S} = \sigma^{\text{signal}}\sqrt{\text{L}}/\sqrt{\sigma^{\text{bkg}}}$ is also given with the luminosity $\text{L} = 100\ \text{fb}^{-1}$. After all the selection cuts, we can see that with $\text{L} = 100\ \text{fb}^{-1}$ the total number of events for the prompt $t\bar{t}J/\psi$ production with the subsequent decay $J/\psi \to \mu^+\mu^-$ can account for more than 600 and the corresponding significance can reach more than 100. The reason for the decline of the significance after the cut (13) is that the contributions from the lower $p_T^{J/\psi}$ region dominate, which can be seen in the Fig. 2. Therefore, we suggest that the $p_T^{J/\psi}$ should be measured as lower as the experiment can to get larger significance and more signal events.

B. Unstable top quarks

Then we continue our discussion including top quark decays. For both the signal and background, the top quarks also decay using NWA method with $\text{BR}(t \to Wb) = 100\%$; both W bosons, resulting from the top-quark decays, are required to decay leptonically or hadronically with $\text{Br}(W \to e\nu) = 10.71\%$, $\text{Br}(W \to \mu\nu) = 10.63\%$ and $\text{Br}(W \to qq') = 67.41\%$ [41].

1. $t\bar{t}J/\psi$ production in tetralepton channel at the LHC

First, we consider that all the top quarks leptonically decay, which will bring out the tetralepton signatures with the process $pp \to (t \to W^+(\ell^+\nu)b)(\bar{t} \to W^-(\ell^-\bar{\nu})\bar{b}) \times (J/\psi \to \mu^+\mu^-)$. All the corresponding possible tetralepton channels are listed in Table VI. Events should contain two pairs of opposite-sign leptons, and at least one pair must be mouns. Since we simply analyze the signatures at the production level, the backgrounds with the same final states for tetralepton signature are considered. The process $pp \to t\bar{t}\mu^+\mu^-$ with top quark subsequent decays contribute dominantly. We find that the contributions from other backgrounds, such as four bosons production process $pp \to V_1V_2V_3V_4 \to \mu^+\mu^-\ell^+\ell^-\nu\bar{\nu}b\bar{b}$, can be neglected.

For the channels listed in Table VI, all the final leptons in the signal and background events satisfy the following cuts:

$$p_T^{\ell^\pm} > 2.5\ \text{GeV}, \quad |\eta_{\ell^\pm}| < 2.3,$$
$$|m(\mu^+\mu^-) - m_{J/\psi}| < 0.5\ \text{GeV},$$
$$8.5\ \text{GeV} < p_T^{J/\psi} < 30\ \text{GeV}, \quad |y_{J/\psi}| < 2.1 \tag{15}$$

in the following analyses according to the Sec. IV A, where the J/ψ mesons are reconstructed from one pair of opposite charge muons. In case the event includes more than one such muon pair, the pair with an invariant mass closet to the nominal value of $m_{J/\psi}$ is attributed to J/ψ mesons and selected to reconstruct the J/ψ meson candidate. The two remaining leptons are considered as top quark decay candidates. The efficiency ϵ_b we used to correctly tag a b-quark jet is approximately 77%, as determined for b-jets with

$$p_T^b > 20\ \text{GeV}, \qquad |\eta_b| < 2.5 \tag{16}$$

in simulated $t\bar{t}$ events [62]. In this paper, only b-jets satisfy the cuts (16) are selected.

In Table VII, we list the total cross section for the signal of direct and indirect J/ψ production and the SM background in the tetralepton channels after considering the cuts (15) and (16) and the b-tagging efficiency. We also list the prompt production J/ψ significance in the last column with the luminosity $\text{L} = 100\ \text{fb}^{-1}$. We can see that for the prompt J/ψ production in all the tetralepton channels the significances are all more than 5 with $\text{L} = 100\ \text{fb}^{-1}$. At the future HL-LHC with $\text{L} = 3000\ \text{fb}^{-1}$, prompt J/ψ production in associated with top quark pair can cumulate about more than 300 events in the tetralepton channel.

2. $t\bar{t}J/\psi$ production in trilepton channel at the LHC

In this part, we focus on the production rate of $t\bar{t}J/\psi$ events measured for the final state with three leptons in the

TABLE VII. The cross sections (in unit of fb) for the signal from the direct and prompt J/ψ production and background in the tetralepton channels at the 13 TeV LHC. The significances with $\text{L} = 100\ \text{fb}^{-1}$ are also given.

		Indirect						
Channels\Source	Direct	From $\psi(2S)$	From χ_{c2}	From χ_{c1}	From χ_{c0}	Total indirect	Background	$\mathcal{S}$
$2\mu 2e 2b + \not{E}_T$	0.019	0.0021	0.0035	0.0038	0.00005	0.0095	0.0015	7.4
$3\mu 1e 2b + \not{E}_T$	0.038	0.0042	0.0071	0.0077	0.00010	0.019	0.0032	10.1
$4\mu 2b + \not{E}_T$	0.019	0.0021	0.0035	0.0038	0.00005	0.0095	0.0016	7.1
Combined	0.076	0.0084	0.0141	0.0153	0.00020	0.038	0.0063	14.4

TABLE VIII. List of the trilepton channels for $t\bar{t}J/\psi$ production. The symbols b and ν denote a b-quark or antiquark and neutrino or antineutrino, respectively, with charge conjugation implied.

$t\bar{t}$ decay	J/ψ decay	Channel
$(qq'b)(e\nu b)$	$\mu^+\mu^-$	$2\mu 1e 2b + \not{E}_T$
$(qq'b)(\mu\nu b)$	$\mu^+\mu^-$	$3\mu 2b + \not{E}_T$

process $pp \to (t \to W(qq')b)(t \to W(\ell\nu)b)(J/\psi \to \mu^+\mu^-)$, where one top quark decays hadronically and the other leptonically. We list all the corresponding possible trilepton channels in Table VIII. Events should contain three leptons, and at least one pair of opposite-sign muons. Similar as the tetralepton channel, we also only consider the dominant contribution from the process $pp \to t\bar{t}\mu^+\mu^-$ with top quark subsequent decays. We also use the cut (15) for the final leptons and J/ψ, cut (16) for final b-jets and the b-tagging efficiency $\epsilon_b = 77\%$. In the $3\mu 2b + \not{E}_T$ channel, the opposite-sign muon pair with an invariant mass closet to $m_{J/\psi}$ is selected to reconstruct the J/ψ meson candidate. In Table IX, we summarize the contributions for the total cross section from the signal of J/ψ produced directly and indirectly after the selection cuts and the b-tagging efficiency, respectively. The corresponding irreducible background production rates and the prompt J/ψ significances with $\mathrm{L} = 100\ \mathrm{fb}^{-1}$ are also listed there. We can see that the direct contribution for the prompt J/ψ production in the trilepton channel at 13 TeV LHC can account for about 0.53 fb, and the indirect contribution is half of the direct.

V. DISCUSSION AND SUMMARY

In this paper, we investigate the prompt J/ψ production in associated with top quark pair to LO in the NRQCD factorization formalism at the 13 TeV LHC. The prompt J/ψ candidates can be produced directly and indirectly. The contributions for the indirect J/ψ production come from radiative decays of $\chi_{cJ} \to J/\psi + \gamma$ or hadronic decays of $\psi' \to J/\psi + X$. We present the total and differential cross section for the direct and indirect J/ψ production with the basic cut $p_T^{\mathcal{Q}} > 3$ GeV. We find that the prompt production rates can account for more than 1100 fb and the Fock state $^3S_1^{(8)}$ gives the dominate contribution to the total and differential cross section.

Then we present the analyses of the prompt $t\bar{t}J/\psi$ signatures at the LHC. We consider the J/ψ decaying into a pair of muons, and take the $pp \to t\bar{t}\mu^+\mu^-$ process as the irreducible background. We begin our studies with stable top quarks, and implement the kinematic cuts for the final reconstructed J/ψ mesons with $p_T^{J/\psi} > 8.5$ GeV and $|y_{J/\psi}| < 2.1$, which were used in the ATLAS experiments before. Through the investigation of the normalized distributions of the p_T^t, $p_T^{J/\psi}$ and $M_{t\bar{t}}$, we can get the maximum significance for the prompt J/ψ production with addition cuts of $p_T^{J/\psi} < 30$ GeV. In this situation, we can get more than 600 prompt $t\bar{t}J/\psi$ events at 13 TeV LHC with $\mathrm{L} = 100\ \mathrm{fb}^{-1}$ via the decay channel $J/\psi \to \mu^+\mu^-$.

Furthermore, we consider the top quarks decay leptonically or hadronically, and analyze prompt $t\bar{t}J/\psi$ production in the tetralepton and trilepton channels at the LHC with the processes $pp \to (t \to W^+(\ell^+\nu)b)(\bar{t} \to W^-(\ell^-\bar{\nu})\bar{b})(J/\psi \to \mu^+\mu^-)$ and $pp \to (t \to W(q\bar{q})b)(t \to W(\ell\nu)b)(J/\psi \to \mu^+\mu^-)$. In the tetralepton channels, we find that the prompt significance can all be more than 5 with $\mathrm{L} = 100\ \mathrm{fb}^{-1}$, and at the future HL-LHC with $\mathrm{L} = 3000\ \mathrm{fb}^{-1}$, the total number of events can account for more than 300. In the trilepton channels, the prompt production rates for $t\bar{t}J/\psi$ at 13 TeV LHC can cumulate about 0.53 fb. We can find that the $t\bar{t}J/\psi$ production at the LHC have the potential to be detected. The measurement of the production J/ψ in associated with top quark pair is useful to investigate the production mechanism of the heavy quarkonium and deepen our understanding about the strong interaction.

In our paper, we only estimated the LO NRQCD contribution for the prompt J/ψ production in associated with top pair. For the process, the uncertainties of the results not only from the LDMEs, but also from the choices of heavy quark mass and the effects of the relativistic correction and higher order correction. It is common knowledge that the relativistic correction [63–65] and higher order correction [66,67] may give considerable contribution for production of the heavy quarkonium production processes, further investigations for relativistic correction and high order correction to the process of heavy quarkonium association with top pair production are significative work.

TABLE IX. The cross sections (in unit of fb) for the signal from the direct and prompt J/ψ production and background in the trilepton channels at the 13 TeV LHC. The significances with $\mathrm{L} = 100\ \mathrm{fb}^{-1}$ are also given.

		Indirect						
Channels\Source	Direct	From $\psi(2S)$	From χ_{c2}	From χ_{c1}	From χ_{c0}	Total indirect	Background	$\mathcal{S}$
$2\mu 1e 2b + \not{E}_T$	0.266	0.0292	0.050	0.054	0.00073	0.134	0.020	28.3
$3\mu 2b + \not{E}_T$	0.264	0.0289	0.049	0.053	0.00073	0.132	0.021	27.3
Combined	0.530	0.0581	0.099	0.107	0.00146	0.266	0.041	39.3

ACKNOWLEDGMENTS

We thank Jinmian Li and Ze-Bo Tang for helpful discussions. This work was supported in part by the National Natural Science Foundation of China (Grants No. 11805001, No. 11305001, No. 11575002, No. 11675033, and No. 11747317) and the Key Research Foundation of the Education Ministry of Anhui Province of China (Grant No. KJ2017A032).

[1] G. T. Bodwin, E. Braaten, and G. P. Lepage, Phys. Rev. D **51**, 1125 (1995); **55**, 5853(E) (1997).
[2] G. P. Lepage, L. Magnea, C. Nakhleh, U. Magnea, and K. Hornbostel, Phys. Rev. D **46**, 4052 (1992).
[3] R. Aaij *et al.* (LHCb Collaboration), Phys. Lett. B **707**, 52 (2012).
[4] R. Aaij *et al.* (LHCb Collaboration), J. High Energy Phys. 06 (2017) 047; 10 (2017) 068(E).
[5] V. M. Abazov *et al.* (D0 Collaboration), Phys. Rev. D **90**, 111101 (2014).
[6] V. Khachatryan *et al.* (CMS Collaboration), J. High Energy Phys. 09 (2014) 094.
[7] M. Aaboud *et al.* (ATLAS Collaboration), Eur. Phys. J. C **77**, 76 (2017).
[8] G. Aad *et al.* (ATLAS Collaboration), Eur. Phys. J. C **75**, 229 (2015).
[9] G. Aad *et al.* (ATLAS Collaboration), J. High Energy Phys. 04 (2014) 172.
[10] R. Aaij *et al.* (LHCb Collaboration), J. High Energy Phys. 06 (2012) 141; 03 (2014) 108(A).
[11] J. P. Lansberg and H. S. Shao, Phys. Rev. Lett. **111**, 122001 (2013).
[12] J. P. Lansberg and H. S. Shao, Phys. Lett. B **751**, 479 (2015).
[13] J. P. Lansberg and H. S. Shao, Nucl. Phys. **B900**, 273 (2015).
[14] J. P. Lansberg, C. Pisano, F. Scarpa, and M. Schlegel, Phys. Lett. B **784**, 217 (2018); **791**, 420(E) (2019).
[15] L. P. Sun, H. Han, and K. T. Chao, Phys. Rev. D **94**, 074033 (2016).
[16] A. K. Likhoded, A. V. Luchinsky, and S. V. Poslavsky, Phys. Rev. D **94**, 054017 (2016).
[17] B. A. Kniehl, C. P. Palisoc, and L. Zwirner, Phys. Rev. D **66**, 114002 (2002).
[18] M. Song, W. G. Ma, G. Li, R. Y. Zhang, and L. Guo, J. High Energy Phys. 02 (2011) 071; 12 (2012) 010(E).
[19] B. Gong, J. P. Lansberg, C. Lorce, and J. Wang, J. High Energy Phys. 03 (2013) 115.
[20] J. P. Lansberg and H. S. Shao, J. High Energy Phys. 10 (2016) 153.
[21] G. Li, M. Song, R. Y. Zhang, and W. G. Ma, Phys. Rev. D **83**, 014001 (2011).
[22] J. P. Lansberg, H. S. Shao, and N. Yamanaka, Phys. Lett. B **781**, 485 (2018).
[23] R. Li and J. X. Wang, Phys. Lett. B **672**, 51 (2009).
[24] J. P. Lansberg, Phys. Lett. B **679**, 340 (2009).
[25] R. Li and J. X. Wang, Phys. Rev. D **89**, 114018 (2014).
[26] S. P. Baranov, Phys. Rev. D **73**, 074021 (2006).
[27] P. Artoisenet, eConf C **0706044**, 21 (2007).
[28] C. F. Qiao, J. Phys. G **29**, 1075 (2003).
[29] J. P. Lansberg, Eur. Phys. J. C **61**, 693 (2009).
[30] P. Artoisenet, J. P. Lansberg, and F. Maltoni, Phys. Lett. B **653**, 60 (2007).
[31] G. Li, S. Wang, M. Song, and J. Lin, Phys. Rev. D **85**, 074026 (2012).
[32] G. Aad *et al.* (ATLAS Collaboration), Phys. Rev. D **91**, 072007 (2015).
[33] M. Aaboud *et al.* (ATLAS Collaboration), J. High Energy Phys. 11 (2017) 086.
[34] A. M. Sirunyan *et al.* (CMS Collaboration), J. High Energy Phys. 10 (2017) 006.
[35] G. Aad *et al.* (ATLAS Collaboration), J. High Energy Phys. 11 (2015) 172.
[36] M. Aaboud *et al.* (ATLAS Collaboration), Eur. Phys. J. C **77**, 40 (2017).
[37] V. Khachatryan *et al.* (CMS Collaboration), J. High Energy Phys. 01 (2016) 096.
[38] A. M. Sirunyan *et al.* (CMS Collaboration), J. High Energy Phys. 08 (2018) 011.
[39] M. Aaboud *et al.* (ATLAS Collaboration), Phys. Lett. B **784**, 173 (2018).
[40] A. M. Sirunyan *et al.* (CMS Collaboration), Phys. Rev. Lett. **120**, 231801 (2018).
[41] M. Tanabashi *et al.* (Particle Data Group), Phys. Rev. D **98**, 030001 (2018).
[42] A. Petrelli, M. Cacciari, M. Greco, F. Maltoni, and M. L. Mangano, Nucl. Phys. **B514**, 245 (1998).
[43] J. Pumplin, D. R. Stump, J. Huston, H. L. Lai, P. M. Nadolsky, and W. K. Tung, J. High Energy Phys. 07 (2002) 012.
[44] T. Hahn, Comput. Phys. Commun. **140**, 418 (2001).
[45] V. Shtabovenko, R. Mertig, and F. Orellana, Comput. Phys. Commun. **207**, 432 (2016).
[46] F. Feng and R. Mertig, arXiv:1212.3522.
[47] T. Hahn and M. Perez-Victoria, Comput. Phys. Commun. **118**, 153 (1999).
[48] S. Fleming and T. Mehen, Phys. Rev. D **57**, 1846 (1998).
[49] B. A. Kniehl and L. Zwirner, Nucl. Phys. **B621**, 337 (2002).
[50] B. A. Kniehl and C. P. Palisoc, Eur. Phys. J. C **48**, 451 (2006).
[51] E. J. Eichten and C. Quigg, Phys. Rev. D **52**, 1726 (1995).
[52] Y. Q. Ma, K. Wang, and K. T. Chao, Phys. Rev. D **83**, 111503 (2011).
[53] G. Li, X.-A. Pan, M. Song, and Y. Zhang (to be published).
[54] M. Butenschoen and B. A. Kniehl, Nucl. Phys. B, Proc. Suppl. **222–224**, 151 (2012).
[55] K. T. Chao, Y. Q. Ma, H. S. Shao, K. Wang, and Y. J. Zhang, Phys. Rev. Lett. **108**, 242004 (2012).

[56] B. A. Kniehl and G. Kramer, Eur. Phys. J. C **6**, 493 (1999); G. Li, M. Song, R. Y. Zhang, and W. G. Ma, Phys. Rev. D **83**, 014001 (2011).
[57] E. Braaten, B. A. Kniehl, and J. Lee, Phys. Rev. D **62**, 094005 (2000).
[58] R. Aaij *et al.* (LHCb Collaboration), Eur. Phys. J. C **75**, 311 (2015); Z. Sun, X. G. Wu, and H. F. Zhang, Phys. Rev. D **92**, 074021 (2015); H. F. Zhang, Z. Sun, W. L. Sang, and R. Li, Phys. Rev. Lett. **114**, 092006 (2015); Z. Sun and H. F. Zhang, Chin. Phys. C **42**, 043104 (2018).
[59] P. L. Cho and A. K. Leibovich, Phys. Rev. D **53**, 150 (1996); E. Braaten and T. C. Yuan, Phys. Rev. D **52**, 6627 (1995); F. Yuan, C. F. Qiao, and K. T. Chao, Phys. Rev. D **56**, 321 (1997).
[60] D. Bertsche, J/psi meson production in association with a W boson: Cross section ratio measurement with the ATLAS detector using 8 TeV pp data from the Large Hadron Collider at CERN, http://inspirehep.net/record/1658382.
[61] J. Alwall, R. Frederix, S. Frixione, V. Hirschi, F. Maltoni, O. Mattelaer, H.-S. Shao, T. Stelzer, P. Torrielli, and M. Zaro, J. High Energy Phys. 07 (2014) 079.
[62] ATLAS Collaboration, Optimisation of the ATLAS b-tagging performance for the 2016 LHC Run, Report No. ATL-PHYS-PUB-2016-012, 2016, https://cds.cern.ch/record/2160731.
[63] Y. J. Li, G. Z. Xu, K. Y. Liu, and Y. J. Zhang, J. High Energy Phys. 07 (2013) 051.
[64] Z. G. He, Y. Fan, and K. T. Chao, Phys. Rev. D **75**, 074011 (2007).
[65] A. P. Martynenko and A. M. Trunin, Phys. Rev. D **86**, 094003 (2012).
[66] C. Zhou, M. Song, G. Li, Y. J. Zhou, and J. Y. Guo, Chin. Phys. C **40**, 123105 (2016).
[67] S. Mao, L. Gang, Z. Ya-Jin, G. Jian-You, and M. Zheng-Wei, Phys. Rev. D **91**, 116004 (2015).